

Early Detection of Infarct in Reperfused Canine Myocardium Using ^{99m}Tc -Glucarate

David R. Okada, BA^{1,2}; Gerald Johnson III, PhD²; Zhonglin Liu, MD³; Sonia D. Hocherman, PhD¹; Ban-An Khaw PhD⁴; and Robert D. Okada, MD^{1,2}

¹Department of Biology, University of Tulsa, Tulsa, Oklahoma; ²Department of Medicine, University of Oklahoma School of Medicine, Tulsa, Oklahoma; ³Department of Radiology, University of Arizona, Tucson, Arizona; and ⁴Department of Pharmaceutical Sciences, Northeastern University, Boston, Massachusetts

^{99m}Tc -Glucarate is an infarct-avid imaging agent with the potential for very early detection of myocardial infarction. The purposes of this study using a canine model were to determine (a) the time course of ^{99m}Tc -glucarate uptake and clearance from necrotic and normal myocardium; (b) the ^{99m}Tc -glucarate necrotic-to-normal activity ratio over time; (c) the time course of detectable scan positivity after intravenous administration of the tracer; and (d) the relationship of infarct size determined by triphenyltetrazolium chloride (TTC) staining versus ^{99m}Tc -glucarate imaging *ex vivo*. **Methods:** A 90-min left circumflex coronary artery (LCx) occlusion was followed by 270 min of reperfusion at 100% baseline flow in 6 open-chest, anesthetized dogs. ^{99m}Tc -Glucarate (555 MBq [15 mCi]) was injected 30 min after reperfusion and was followed by 240 min of γ -camera serial imaging. Microspheres were injected during baseline, occlusion, tracer injection, and before the dogs were euthanized. Creatine kinase assays were performed to assess developing injury. *Ex vivo* γ -camera imaging was performed. Blood flow and tracer activity were determined by well counting. TTC stain was used to mark infarct areas, which were sized using computerized digital planimetry. **Results:** Hemodynamics demonstrated no significant change from baseline at any time for any parameter except LCx flow, which was significantly depressed during occlusion. The mean infarct size \pm SEM was 10.7% \pm 2% of total left ventricle. Blood ^{99m}Tc -glucarate clearance was triexponential and rapid. Qualitative image analysis revealed a well defined hot spot after 30 min, which remained well defined through 240 min after injection (150 and 360 min after occlusion, respectively). Images were quantitatively abnormal with hot spot-to-normal zone activity ratios of $\geq 2:1$ within 10 min of tracer administration (130 min after occlusion), reaching 8:1 at 240 min after tracer administration (360 min after occlusion). There was a linear correlation between infarct size determined by ^{99m}Tc -glucarate and TTC staining ($r = 0.96$; slope = 0.87). **Conclusion:** ^{99m}Tc -Glucarate marks acute myocardial infarct very early after occlusion and appears to accurately assess infarct size when compared with TTC staining.

Key Words: ^{99m}Tc -glucarate; imaging; myocardial infarction; radiotracer kinetics

J Nucl Med 2004; 45:655–664

Received Apr. 10, 2003; revision accepted Aug. 14, 2003.
For correspondence or reprints contact: Robert D. Okada, MD, Department of Biology, University of Tulsa, 6208 S. Oswego Ave., Tulsa, OK 74136.
E-mail: rokada576@hotmail.com

Glucarate is a 6-carbon dicarboxylic acid that has been proposed as a potentially useful SPECT imaging agent for acute myocardial infarction. The mechanism of ^{99m}Tc -glucarate uptake and retention in infarcted myocardium is by binding to nuclear histones exposed by cellular and nuclear membrane breaks caused by irreversible myocyte injury (oncosis) (1,2). Several small animal studies have demonstrated increased ^{99m}Tc -glucarate uptake in acutely necrotic myocardium (1,3–7). However, more clinically relevant data from large animal models are limited (3,8).

Accordingly, we studied ^{99m}Tc -glucarate in a well-characterized canine model. The protocol included continuous hemodynamic and epicardial blood flow monitoring, microsphere-determined blood flows, *in vivo* and *ex vivo* γ -camera imaging, creatine kinase (CK) enzyme monitoring, triphenyltetrazolium chloride (TTC) staining, and postmortem γ -well counting of tissues. The aims of this study were to investigate (a) the time course of ^{99m}Tc -glucarate uptake and clearance in normal and necrotic myocardium; (b) the ^{99m}Tc -glucarate necrotic-to-normal activity ratio over time; (c) the time course of scan positivity after intravenous administration of the tracer, and (d) the relationship between infarct size determined by TTC staining versus ^{99m}Tc -glucarate imaging.

MATERIALS AND METHODS

Surgical Preparation and Tracer Preparation

Six adult mongrel dogs (mean weight \pm SEM, 19.2 \pm 1.5 kg; range, 14–23 kg) were anesthetized with sodium pentobarbital (26 mg/kg intravenously). Supplemental anesthetic was administered throughout the experiment as necessary. The dogs were intubated and placed on a ventilator (Harvard Apparatus Co., Inc.) with 95% oxygen. Vinyl catheters were inserted into both femoral arteries to monitor arterial pressure and withdraw blood samples for blood gas determination. Appropriate adjustments were made to maintain pH = 7.35–7.45, partial pressure of CO₂ (P_{CO₂}) = 30–40 mm Hg, and partial pressure of O₂ (P_{O₂}) > 90 mm Hg. The carotid artery was cannulated to provide a site for microsphere reference blood withdrawal. Vinyl catheters were also inserted into both femoral veins as sites for the infusion of radiotracer, supplemental anesthetics, and fluids as required.

The heart was exposed through a left thoracotomy at the fifth intercostal space and suspended in a pericardial cradle. The lungs were carefully moved aside to allow for the pericardial cradle to be sutured to the chest wall. A vinyl catheter was inserted into the left atrial appendage to monitor left atrial pressure and provide a site for the injection of radiolabeled microspheres. A Swan-Ganz thermodilution catheter (Baxter Healthcare Corp.) was inserted into the right jugular vein and passed through the right side of the heart until its tip rested in the pulmonary artery. The catheter was subsequently used for the measurement of cardiac output.

The left circumflex coronary artery (LCx) was then carefully dissected free near the origin and a 2.0- to 2.5-mm transit time flow probe (Transonic Instruments) was placed around the artery. An occluder was positioned distal to the flow probe.

Mean or phasic systemic arterial pressure, left atrial pressure (Statham p23 ID transducers; Gould Electronics), LCx flow, and lead II of the electrocardiogram were monitored continuously throughout the protocol on a computerized chart recorder using commercial software (DataFlow). Thermodilution cardiac outputs and arterial blood gases were monitored throughout the protocol.

Glucurate kits, provided by Molecular Targeting Technology, Inc., each consisted of a lyophilized mixture of sodium glucurate (12.5 mg) and stannous chloride. To each of these kits, 925 MBq (25 mCi) of generator-eluted $^{99m}\text{TcO}_4^-$ were added (Syncor). The reaction among the reagents was allowed to proceed for 30 min at room temperature. To ensure the completeness of reaction, quality control was performed with 3-mm-thick (Whatman) chromatography and developed in saline solution (8.4%). Every kit analyzed demonstrated labeling efficiency of >98%.

Experimental Protocol

Figure 1 illustrates the experimental protocol. Baseline hemodynamic measurements were recorded during a 20-min period after instrumentation in all 6 dogs. After the 20-min baseline, microspheres were injected into the left atrial appendage to determine regional myocardial blood flows. Ten minutes after microsphere injection (and 30 min after instrumentation), the LCx was occluded with a proprietary, precision, plastic screw occluder. Forty-five minutes later, microspheres were again injected into the left atrial appendage. The ultrasonic transit time flow probe was used to confirm stable coronary occlusion.

Forty-five minutes later (90 min after beginning the occlusion), the arterial clamp on the LCx was loosened to provide 100% reperfusion. Reactive hyperemia was prevented by gradually loosening the arterial clamp until baseline flow was achieved by flow meter. At 120 min after initial occlusion (30 min after reperfusion),

555 MBq (15 mCi) ^{99m}Tc -glucurate were injected into the right femoral vein. The exact dose was calculated by measuring the activity in the syringe before and after injection using a dose calibrator. Simultaneously, a third microsphere blood flow determination was performed. This microsphere flow determination, along with the ultrasonic transit time probe, was used to confirm 100% reflow. In vivo planar images were acquired as detailed below over the subsequent 4-h period.

To measure blood ^{99m}Tc -glucurate activity during the 4-h reperfusion period, 1.0-mL serial arterial blood aliquots were collected at 0.5, 1, 1.5, 2, 4, 6, 8, 10, 20, 30, 60, 90, 120, 150, 180, 210, and 240 min after tracer injection. At the end of the study period (240 min after ^{99m}Tc -glucurate injection), a final myocardial blood flow determination was made by injecting a fourth set of microspheres. The dogs were then euthanized. The order in which radiolabeled microspheres were injected was randomized during the study to prevent bias.

In Vivo γ -Camera Imaging Protocol

In vivo scintigraphic planar images were obtained with a mobile γ -camera (model 420; Ohio-Nuclear Inc.) interfaced with a Pegasus nuclear imaging computer system (ADAC Laboratories). A high-resolution collimator was used in conjunction with a 20% energy window encompassing the 140-keV ^{99m}Tc photopeak. Imaging was performed in the left lateral projection. An arrangement of 3 pieces of lead shielding was placed under the heart and over the abdomen of each dog to eliminate any contribution of liver and gut activity to the images. Three dynamic images were collected in a $128 \times 128 \times 8$ matrix with the following image timing: 15×4 s per frame, 54×15 s per frame, 5×60 s per frame. Static images were collected in a $128 \times 128 \times 16$ matrix from 30 to 240 min after tracer administration using a 300-s acquisition time. Once established, the position of the camera head in relation to the preparation was not altered.

Myocardial Viability Assessment (CK Assay)

Ongoing cardiomyocyte injury was assessed by measurement of CK activity in blood. One-milliliter samples of venous blood were collected at 120 min before occlusion, at occlusion, and at 45, 90, 100, 110, 120, 180, 240, 300, and 360 min after occlusion. The CK concentration (U/L) was measured using a spectrophotometer (model DU640; Beckman Co.) and CK assay kits (Sigma). These kits were not specific for canine CK-MB as they measured all CK isoforms. Therefore, we acquired 2 baselines, one before surgery and one after surgery so that we could assess injury due to surgery separately from injury due to infarct.

Postmortem Ex Vivo Analysis

Postmortem, hearts were removed quickly, atria and great vessels were removed, and the left ventricle was sliced into four 1-cm slices from apex to base. The slices were imaged on the face of the γ -camera, then were stained with TTC, and photographed as described. Each slice was then further divided radially into 8 equal sections. These sections and the ^{99m}Tc -glucurate blood aliquots were counted for 2 min each in a γ -well counter (model 1282; LKB Instruments) with a 120- to 160-keV window to detect ^{99m}Tc activity. These count data from the γ -well counter were corrected for background, radioactive decay, and spill-down activities from the microspheres. After ^{99m}Tc decay (3 d), the microsphere reference blood samples and the same myocardial tissue samples were again counted for 5 min each using windows as described.

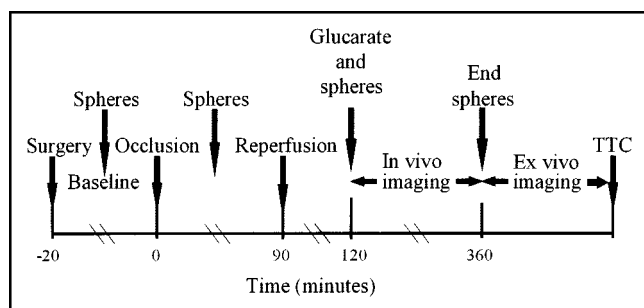


FIGURE 1. Experimental protocol. Time line shows both the order of procedural events and the time between or allotted to each of these events.

Microspheres were labeled with ^{113}Sn , ^{103}Ru , ^{95}Nb , or ^{46}Sc . The microsphere technique has been used widely in our laboratory and has been described previously (9).

Appropriate window settings were chosen for each isotope (^{113}Sn was counted within a 350- to 435-keV window, ^{103}Ru within a 450- to 550-keV window, ^{95}Nb within a 660- to 800-keV window, and ^{46}Sc within an 810- to 1,200-keV window). A computer was used to correct for both background and spillover of activity from one window into another and to calculate regional myocardial blood flow with proprietary software developed in our laboratory for this purpose. Regional myocardial blood flow was expressed as milliliters per minute per gram of tissue as calculated from the microsphere count data and tissue sample weights. Myocardial blood flow ratios were calculated by dividing the flow in the left circumflex (occlusion) zone by the flow in the left anterior descending coronary (control) zone.

Ex Vivo γ -Camera Imaging and Myocardial Viability Assessment (TTC Staining)

After euthanasia, the left ventricle was initially sectioned into 4 slices as discussed above. The γ -camera was positioned such that it faced upward. Each myocardial slice was placed on the face of the γ -camera head. Images were obtained for 600 s.

TTC staining was then used to determine myocardial tissue viability. After ex vivo γ -camera imaging, the tissues were incubated in the TTC Tris solution, pH 7.8, at 37°C for 15 min. The 4 TTC-stained myocardial slices were photographed and quantitatively analyzed using video densitometry software (SigmaScan) to calculate the percentage of viable myocardium. Care was taken to maintain the same orientation used for ex vivo γ -camera imaging.

Data Analysis and Statistical Methods

In vivo and ex vivo images were assessed qualitatively by trained observers, comprised of both clinicians and scientists. The observers reached a consensus regarding the presence or absence of a hot spot.

In vivo images were further assessed quantitatively by defining regions of interest (ROI) in the septal area (left anterior descending artery [LAD] normal zone) and lateral wall (LCx occlusion zone). ROIs were 3 × 3 pixels each. The septal and lateral wall ROIs were placed midway between the base and apex. These ROIs remained constant in size and location, as images taken at several time points were analyzed. Mean counts per pixel in these ROIs were then obtained and the LCx/LAD ratios were calculated for each dog over time. An analysis of each zone was performed separately by determining $^{99\text{m}}\text{Tc}$ activity over time. Washout curves were normalized to peak activity. Activities were corrected for background, $^{99\text{m}}\text{Tc}$ decay, and differences in image acquisition time. Washout curves were normalized for activity measured 10 min after $^{99\text{m}}\text{Tc}$ -glucarate injection to avoid the potential added activity from blood pool and lungs. Fractional myocardial clearance at any time point (up to 240 min) was defined as the difference between the initial counts and subsequent counts divided by the initial counts. These values were expressed as percentages.

Blood clearance curves were modeled using a least-squares nonlinear regression analysis (Tablecurve for Windows; SPSS, Inc.).

Ex vivo images were further assessed quantitatively. Myocardial $^{99\text{m}}\text{Tc}$ -glucarate hot spot area was determined by video computerized densitometry. Hot spot area was expressed as a percentage of the total left ventricular area. The infarct sizes calculated from the ex vivo γ -camera images and those calculated from the

TTC staining were then compared using a linear regression analysis.

All results were expressed as a mean \pm SEM. The significance of mean differences between groups was assessed using a 1-way repeated measures ANOVA when comparing either results at different times or different regions of the same heart. Differences in flow in different areas of the heart at different times were analyzed using a 2-way repeated ANOVA (by time and by region). Post hoc comparisons were made using *t* tests with correction for multiple comparisons made by the Bonferroni procedure (SigmaStat; SPSS, Inc.). All *P* values < 0.05 were considered significant.

Animal Treatment

All experimental animals were handled in accordance with the guiding principles of the American Physiological Society and the Institutional Animal Care and Use Committee of the University of Oklahoma Health Sciences Center.

RESULTS

Hemodynamics, Microsphere Blood Flows, and CK Assay

Table 1 lists the hemodynamic data. There were no significant changes in mean arterial pressure, systolic arterial pressure, left atrial pressure, and mean heart rate over time. LCx flow by transit time flow probe fell to zero during coronary occlusion and recovered to baseline immediately after reperfusion.

Table 2 lists the myocardial blood flows for the individual dogs. There was a significant difference between LAD and LCx mean flows during LCx occlusion. However, there were no significant differences between LAD and LCx mean flows at baseline, during reperfusion, and at the end of the experiment.

Figure 2 illustrates CK activity (U/L) over time in minutes. As expected, CK activity increased slightly, but not significantly, immediately after surgery. After LCx occlusion, CK activity began a significant increase from baseline 2, which continued from reperfusion until the end of the study. These data were used to assess the ongoing development of infarct after reperfusion.

$^{99\text{m}}\text{Tc}$ -Glucarate Blood Kinetics

Figure 3 illustrates $^{99\text{m}}\text{Tc}$ -glucarate mean blood clearance data over time normalized to percent peak. Blood clearance was qualitatively rapid. Quantitatively, fractional retention was only 6.5% \pm 1.6% peak at 30 min, and 1.9% \pm 0.4% peak at 240 min after injection. The blood clearance was best fit to a triexponential function. The equation was $f = a \cdot \exp(-b \cdot x) + c \cdot \exp(-d \cdot x) + g \cdot \exp(-h \cdot x)$, where $a = 337,039.32$, $b = 17.72$, $c = 48.25$, $d = 0.24$, $g = 9.75$, $h = 0.01$ ($r = 0.99$; $F = 2,330$).

Qualitative Image Analysis

When the in vivo γ -camera images were assessed by 2 trained observers, 6 of 6 dogs were determined to have developed clear and distinct left ventricular hot spots within 30 min of $^{99\text{m}}\text{Tc}$ -glucarate administration (150 min after occlusion)

TABLE 1
Hemodynamic Data

Hemodynamic data	Dog 1	Dog 2	Dog 3	Dog 4	Dog 5	Dog 6	Mean \pm SEM
Cardiac output (L/min)							
Baseline	2.7	4.2	3.5	3.9	2.6	2.3	3.2 \pm 0.3
Occlusion	2.8	3.7	3.8	3.6	1.6	2.0	3.0 \pm 0.3
Reperfusion	2.9	2.7	3.1	3.0	2.2	3.0	2.8 \pm 0.1
End	1.5	3.5	2.7	2.9	1.9	2.8	2.5 \pm 0.2
LCx epicardial flow (mL/min)							
Baseline	25	39	20	19	27	44	29 \pm 4
Occlusion	0	0	0	0	0	0	0* \pm 0
Reperfusion	25	39	13	18	25	44	27 \pm 4
End	10	29	10	15	12	30	17 \pm 3
Heart rate (beats/min)							
Baseline	163	111	133	104	133	120	127 \pm 8
Occlusion	162	106	116	112	126	118	123 \pm 8
Reperfusion	168	103	104	113	120	122	122 \pm 9
End	140	95	124	93	128	148	121 \pm 9
Mean left atrial pressure (mm Hg)							
Baseline	0	1.3	1.6	1.1	3.1	4.1	1.9 \pm 0.6
Occlusion	2.5	2.8	4.5	1.0	4.5	5.3	3.4 \pm 0.6
Reperfusion	0.8	4.3	1.5	1.3	5.4	5.6	3.1 \pm 0.8
End	0	0.9	1.2	1.0	18.7	3.5	4.2 \pm 2.9
Mean arterial pressure (mm Hg)							
Baseline	121	112	115	112	101	107	111 \pm 2
Occlusion	113	93	95	120	91	89	100 \pm 5
Reperfusion	109	90	8	132	87	92	99 \pm 7
End	90	81	71	101	98	122	94 \pm 7
Arterial systolic pressure (mm Hg)							
Baseline	140	135	139	119	119	132	131 \pm 3
Occlusion	131	112	110	128	108	113	117 \pm 4
Reperfusion	130	115	101	149	103	121	120 \pm 7
End	108	110	96	112	116	140	114 \pm 5

* $P < 0.0001$ compared with other time points.

(Fig. 4). Hot spots were well visualized on all subsequent images to 240 min after ^{99m}Tc -glucarate administration (360 min after occlusion). For the first 30 min after ^{99m}Tc -glucarate administration, the lateral wall hot spot was present but was difficult to visualize clearly due to blood-pool activity.

Ex vivo images also demonstrated ^{99m}Tc -glucarate hot spots in 6 of 6 dogs. All hot spots were confined to the lateral wall.

Quantitative Image Analysis

Regional ^{99m}Tc -glucarate clearance curves derived from serial in vivo γ -camera images obtained at 1, 10, 30, 60, 90, 120, 150, 180, 210, and 240 min were normalized to peak activity and then plotted (Fig. 5). Beginning at 10 min after tracer injection (130 min after occlusion) and continuing through the remainder of the study period, ^{99m}Tc -glucarate activity (% peak) was significantly lower for the LAD control than for the LCx hot spot zones ($P < 0.05$). At 240 min after tracer injection (360 min after occlusion), the fractional retention was 18.4% \pm 1.2% for the LAD control zone versus 73.4% \pm 9.7% for the LCx hot spot zone ($P < 0.05$).

γ -Camera ^{99m}Tc count ratios of the LCx hot spot to LAD control zones plotted over time are shown in Figure 6. The

ratio began to rise immediately after tracer injection. Within 10 min after tracer injection (130 min after occlusion), differential washout created a counts ratio of at least 2:1 for all dogs. At the end of the 240-min posttracer injection study period (360 min after occlusion), this ratio had increased to at least 8:1 for all dogs.

Infarct Size Determination by ^{99m}Tc -Glucarate Versus TTC Staining

Figure 7 shows an ex vivo γ -camera image and TTC stain image from a single heart. When the infarct size calculated from γ -camera imaging was compared with that from TTC staining using linear regression analysis, the Pearson correlation coefficient was $r = 0.96$ and the slope was 0.87.

DISCUSSION

^{99m}Tc -Glucarate is a new myocardial imaging agent developed for the clinical detection of acute myocardial infarction. Only low levels of ^{99m}Tc -glucarate have been noted in normal myocardium. Some investigators have proposed that the mechanism of uptake in normal myocardium may be related to glucarate being transported as a glucose analog (4,10,11). ^{99m}Tc -Glucarate demonstrates enhanced myocar-

TABLE 2
Blood Flows (mL/min/g) and End ^{99m}Tc Activities

Dog	Baseline flow		Occlusion flow		Reperfusion flow		End flow		End activity (%ID/(g × 10 ⁻³))		End activity ratio LCx/LAD	Occlusion flow ratio LCx/LAD
	LAD	LCx	LAD	LCx	LAD	LCx	LAD	LCx	LAD	LCx		
1	1.25 ± 0.03	1.05 ± 0.03	1.29 ± 0.03	0.41 ± 0.07	1.44 ± 0.04	1.03 ± 0.04	0.94 ± 0.03	0.45 ± 0.03	3.4 ± 0.1	15.2 ± 1.8	4.5	0.32
2	1.64 ± 0.04	1.47 ± 0.05	1.03 ± 0.03	0.27 ± 0.04	1.11 ± 0.03	1.27 ± 0.08	0.82 ± 0.02	0.70 ± 0.04	3.0 ± 0.4	20.1 ± 2.8	6.6	0.26
3	1.17 ± 0.04	1.19 ± 0.04	0.95 ± 0.03	0.63 ± 0.08	0.67 ± 0.02	0.80 ± 0.04	0.63 ± 0.01	0.54 ± 0.03	1.3 ± 0.1	3.7 ± 0.5	2.8	0.67
4	0.70 ± 0.02	0.72 ± 0.03	0.77 ± 0.02	0.44 ± 0.04	0.83 ± 0.02	0.72 ± 0.03	0.67 ± 0.02	0.52 ± 0.03	1.0 ± 0.1	4.8 ± 1.0	4.8	0.57
5	1.09 ± 0.03	0.89 ± 0.02	0.78 ± 0.02	0.21 ± 0.04	0.82 ± 0.02	0.86 ± 0.06	0.66 ± 0.01	0.43 ± 0.02	3.3 ± 0.2	8.3 ± 1.2	2.5	0.27
6	1.45 ± 0.06	1.55 ± 0.05	1.23 ± 0.03	0.38 ± 0.07	1.96 ± 0.05	1.78 ± 0.09	1.09 ± 0.03	0.88 ± 0.03	3.0 ± 0.3	15.5 ± 2.3	5.2	0.31
All dogs	1.22 ± 0.13	1.15 ± 0.13	1.01 ± 0.09	0.39 ± 0.06*	1.14 ± 0.20	1.08 ± 0.16	0.80 ± 0.08	0.60 ± 0.07	2.5 ± 0.4	11.3 ± 2.7	4.4 ± 0.6	0.40 ± 0.07

**P* ≤ 0.001 compared with LAD.

End activity is expressed as percentage of injected dose per gram of tissue × 10⁻³.

dial retention in experimentally infarcted myocardium (1,3–5,7,8) The mechanism of this increased ^{99m}Tc-glucuronate uptake in infarcted myocardium is thought to be by binding to nuclear histones exposed by membrane breaks caused by irreversible myocyte injury (1,2). ^{99m}Tc-Glucuronate does not appear to demonstrate enhanced myocardial uptake in experimental injury due to apoptosis (12–14).

The aim of the current investigation was to study ^{99m}Tc-glucuronate kinetics and imaging in a large animal model. The model was hemodynamically stable with respect to heart rate, mean and systolic arterial blood pressure, left atrial pressure, and cardiac output. LAD and LCx blood flows were significantly different only during LCx occlusion, as expected. There were no significant differences between LAD and LCx blood flows at baseline, after reperfusion, and at the end of the study. The model produced significant myocardial injury. CK levels were significantly increased in all dogs. Furthermore, TTC staining demonstrated infarcts in all dogs. Infarct size by TTC staining averaged 10.7% ± 1.9% of the total left ventricle.

We found that ^{99m}Tc-glucuronate blood clearance was rapid: 73.5% cleared within 30 min of intravenous tracer administration, and 98.4% cleared by 240 min. Blood clearance was modeled and was found to be triexponential. Previous investigators have injected ^{99m}Tc-glucuronate intravenously in rabbits and reported that the tracer “was observed to clear rapidly from the blood” (1). Other investigators reported biexponential blood clearance rates from swine (15). Half-time was 5.0 min for the first phase and 54.3 min for the second phase.

Quantitative ^{99m}Tc-glucuronate myocardial kinetics have not been previously reported in a large animal model. In the current study, quantitative analysis of the serial ^{99m}Tc-glucuronate images confirmed significant differences in tracer retention in the infarct compared with the control zone. The LCx occlusion zone and LAD normal zone retentions became significantly different at 10 min after tracer administration (130 min after occlusion). These differences in retention persisted until the end of the 240-min posttracer injection monitoring period (360 min after occlusion). Fractional myocardial retention was 73.4% for the LCx occlusion zone and 18.4% for the LAD normal zone by the end of the 240-min posttracer injection imaging period (360 min after occlusion), confirming significant differences in tracer kinetics.

Regarding the ability of ^{99m}Tc-glucuronate imaging to detect myocardial necrosis, and the time course after coronary occlusion, these issues have been previously addressed in only a limited number of large animals (3,8). Orlandi et al. reported 3 dogs undergoing 90 min of coronary occlusion followed by 48 h of reperfusion (8). In vivo imaging was performed in one dog at 24 h after reperfusion (i.e., 25.5 h after occlusion) compared with the current study in which imaging was performed at 2.0 h after occlusion. Images demonstrated a hot spot in this one previously reported dog.

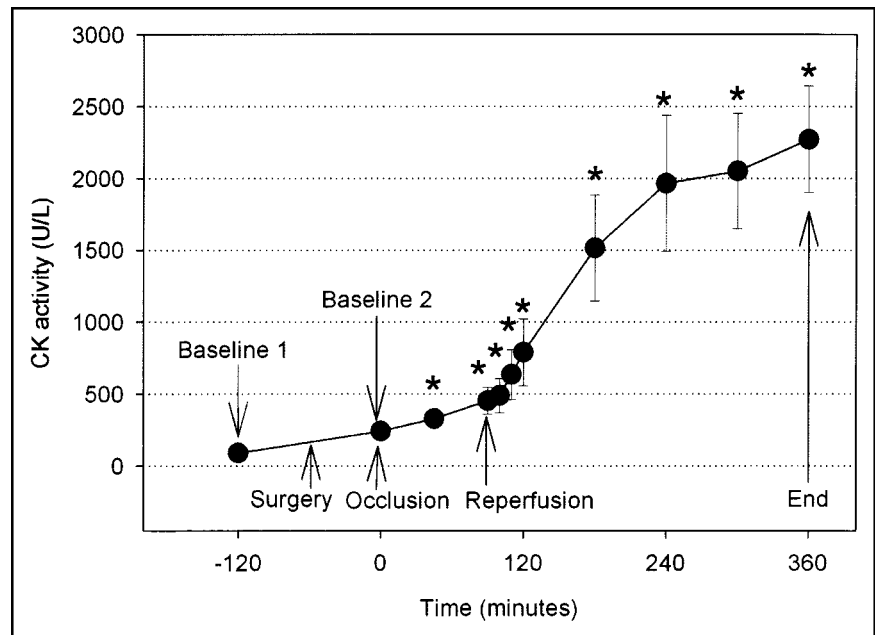


FIGURE 2. Absolute CK activity (U/L) over time. Times corresponding to important procedural events are so marked by an arrow. * $P < 0.05$ from baseline 1.

Quantitative image analysis was not performed. Khaw et al. reported 4 dogs with ^{99m}Tc -glucarate imaging after a 3-h coronary occlusion followed by 4 h of reperfusion (3). All 4 dogs were described qualitatively as having hot spots on in vivo ^{99m}Tc -glucarate images. Ex vivo imaging and quantitative analysis were not reported. That study showed scan positivity at 210 min, in contrast to the current study that found positive tracer uptake at 130 min after coronary occlusion. In the current study, ex vivo γ -camera imaging demonstrated ^{99m}Tc -glucarate hot spots in all dogs. Hot spots were appropriately confined to the lateral left ventricular wall. Unlike ^{99m}Tc -pyrophosphate, the maximal ^{99m}Tc -

glucarate uptake appeared to be in the center of the infarct. In vivo γ -camera images also demonstrated ^{99m}Tc -glucarate hot spots in all dogs. Qualitatively, images first became consistently interpretable at 30 min after intravenous tracer administration (i.e., 150 min after coronary occlusion). However, using quantitative techniques, the LCx occlusion zone-to-normal zone activity ratio began to increase almost immediately after tracer administration and was at least 2:1 by 10 min after tracer administration (i.e., 130 min after coronary occlusion). Thus, this large animal model now demonstrates tracer uptake as early as 130 min after coronary occlusion. It should be noted that the ability of ^{99m}Tc -

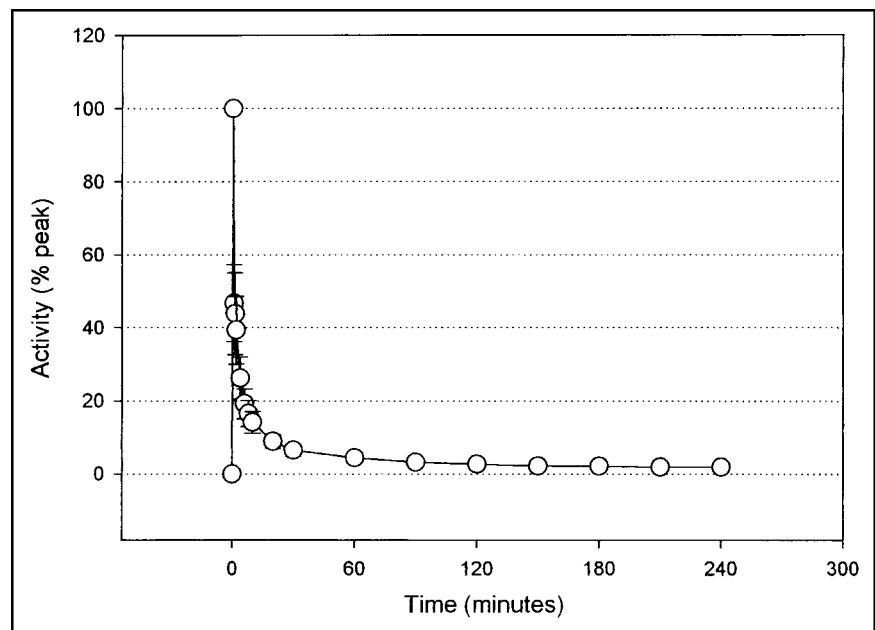


FIGURE 3. ^{99m}Tc -Glucarate blood clearance curve. Activity values are normalized to maximum peak activity and are given as mean \pm SEM for all hearts throughout the protocol. Blood clearance was best fit to triexponential clearance. The equation was $f = a \cdot \exp(-b \cdot x) + c \cdot \exp(-d \cdot x) + g \cdot \exp(-h \cdot x)$, where $a = 337,039.32$, $b = 17.72$, $c = 48.25$, $d = 0.24$, $g = 9.75$, $h = 0.01$ ($r = 0.99$; $F = 2,330$).

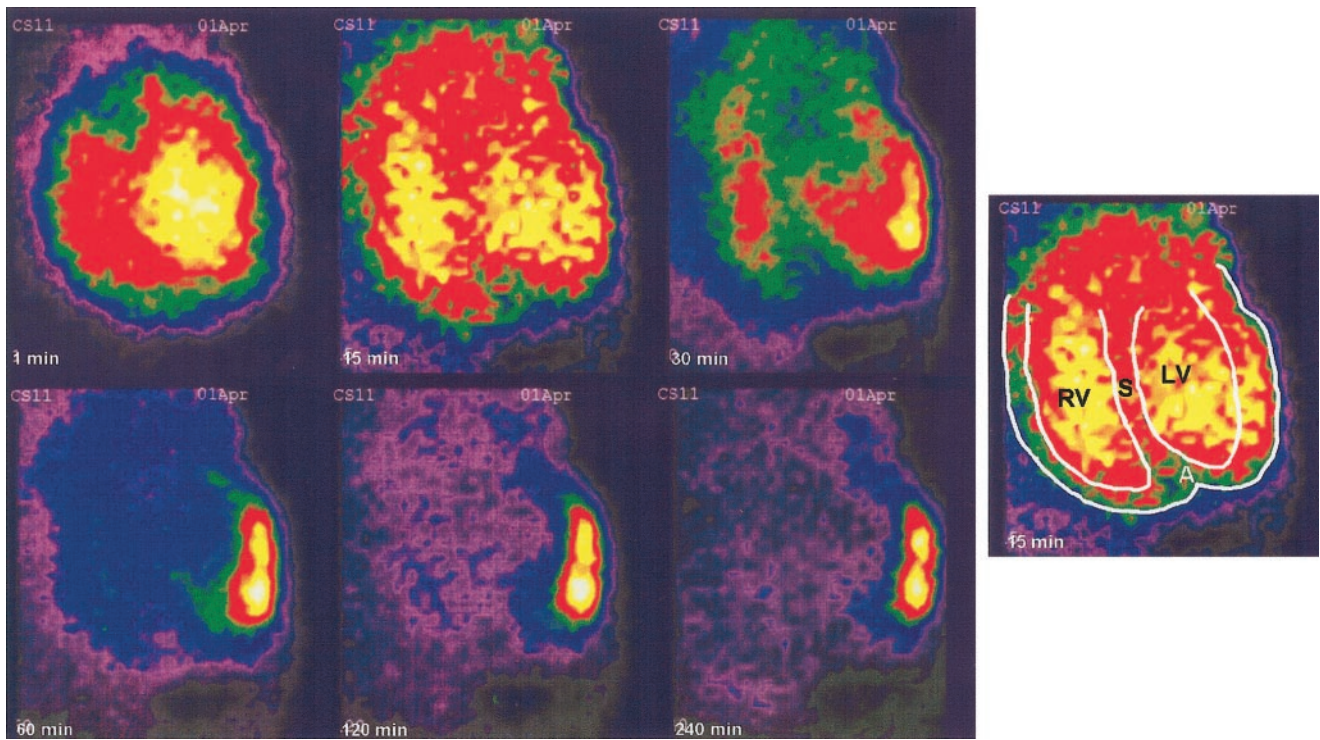


FIGURE 4. In vivo serial γ -camera ^{99m}Tc -glucurate scintigraphic images of single heart, acquired at 1, 15, 30, 60, 120, and 240 min after tracer injection. Hot spot is clearly visualized involving lateral wall at 30 min. RV = right ventricular cavity; S = septum; LV = left ventricular cavity; A = apex of left ventricle.

glucurate to detect infarct was high despite the relatively small size of infarct by TTC. In a clinical study, investigators reported ^{99m}Tc -glucurate imaging results in 28 patients presenting to an emergency room with chest pain suggestive of myocardial infarction (7). Fourteen of 23 patients with myocardial infarction had abnormal images. The earliest positive scan was seen 1 h after the onset of chest pain;

however, most of the positive studies were acquired several hours after the onset of pain.

Regarding the duration of scan positivity, Ohtani et al. studied the time course of scan positivity in a small animal rat model of coronary occlusion using pinhole imaging (5). Images were acquired at 3 h, 24 h, 72 h, and 7–10 d. Ten rats demonstrated no evidence of infarction, and all had

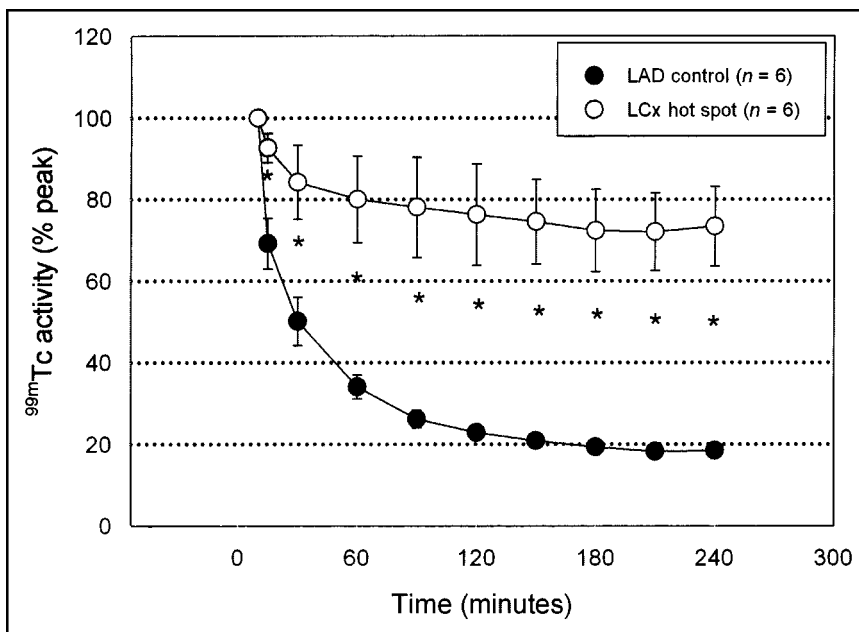


FIGURE 5. ^{99m}Tc -Glucurate retention curves for LAD (control) and LCx (hot spot) territories. Activities were normalized to percentage peak uptake and are given as mean \pm SEM over time. * $P < 0.05$ from LAD control.

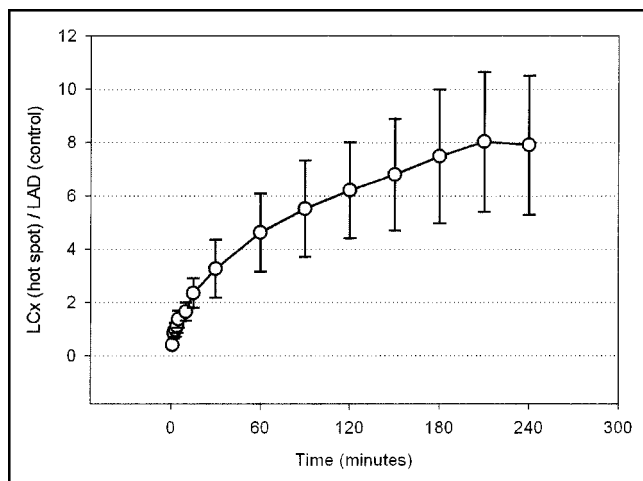


FIGURE 6. LCx/LAD zone ^{99m}Tc -glucarate activity ratio over time.

negative scans. Twenty-one rats demonstrated evidence of infarction and 17 had positive scans. Scan positivity was maximal at 3 h, decreased by 24 h, and was not seen at 72 h and 7–10 d after occlusion. As discussed above, Orlandi et al. reported ^{99m}Tc -glucarate scan positivity at 24 h after coronary occlusion (8). However, 10 d after coronary occlusion, there was no significant tracer uptake. In a study of 28 patients presenting with chest pain, the investigators found the results of ^{99m}Tc -glucarate imaging to be time dependent (7). Fourteen of 14 patients imaged within 9 h of the onset of chest pain had positive scans. However, 9 of 9 patients with infarcts studied >9 h after the onset of chest pain had negative images. Six of 6 patients studied at 6 wk had negative scans. In the current study, ^{99m}Tc -glucarate was administered at 120 min after coronary occlusion. Qualitatively analyzed images persistently demonstrated a hot spot until the end of the 240-min posttracer injection imaging period (360 min after occlusion). Quantitatively, the LCx occlusion-to-LAD normal zone counts ratio increased progressively over the 240-min imaging period. This ratio had increased to 8:1 by 240 min after tracer administration (360 min after coronary occlusion). It was noted that the

ratio started to plateau after 210 min after tracer administration (330 min after coronary occlusion).

One previous investigation studied the time course of scan positivity after intravenous tracer administration in 2 small animal models using rabbits (1). One model involved 40 min of coronary occlusion followed by 45–60 min of reperfusion and then tracer administration. In this model, the authors were able to start visualizing the hot spot within 10 min of intravenous tracer administration. However, hot spots were not consistently visualized until 30 min after tracer administration. In a second model of persistent coronary occlusion, the hot spot could be initially visualized 30 min after intravenous tracer administration. However, hot spots were not consistently visualized until 40–60 min. In a preliminary report, Khaw et al. reported imaging results in rabbits subjected to 45 min of coronary occlusion followed by reperfusion (16). They were able to start visualizing infarcts after only 3–4 min posttracer administration, despite an infarct-to-blood ^{99m}Tc activity ratio of 1.1:1 at the time. Distinct infarct visualization was possible at 10–15 min after tracer administration when infarct-to-blood ^{99m}Tc activity ratios were >1.5:1. In a full report, Khaw et al. were able to visualize infarcts in some dogs starting at 4–10 min after tracer administration (3). However, they were not able to consistently visualize the infarct until 30 min. In the clinical study of patients presenting to the emergency room with chest pain suggestive of myocardial infarction, investigators began γ -camera imaging at 2.0–4.5 h after tracer administration (7). Only 14 of 23 patients with myocardial infarction had positive scans. However, as mentioned above, all 14 of 14 patients with infarcts imaged within 9 h of the onset of chest pain had positive scans. One patient was imaged 24 h after intravenous tracer administration and had a positive scan. In the current study, for the first 30 min after tracer administration, increased activity was qualitatively noted in the lateral wall; however, image quality was degraded by blood-pool activity. By 30 min after tracer administration, the hot spot was easily identified qualitatively. The infarct continued to be well defined until the end of experiment at 240 min after tracer injection. However, using quantitative techniques, enhanced myocardial ^{99m}Tc -

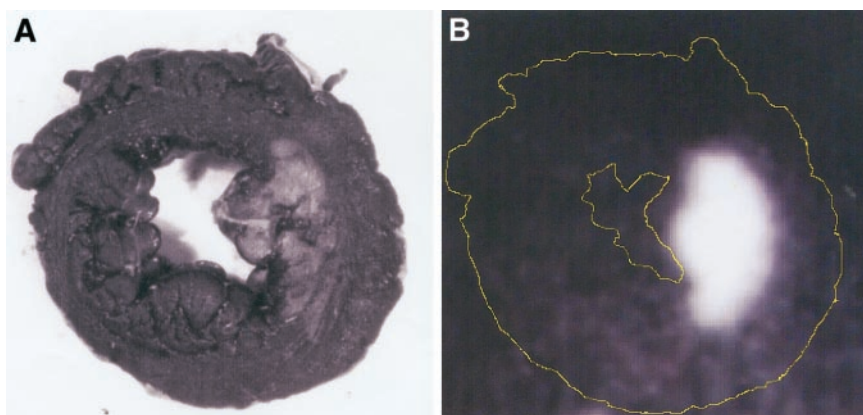


FIGURE 7. (A) Characteristic heart slice photographed after TTC staining. (B) Corresponding ex vivo ^{99m}Tc -glucarate image. Qualitatively, there was good correlation of size, shape, and location.

glucarate retention could be detected much earlier. The LCx occlusion zone-to-LAD normal zone counts ratio began to increase immediately and was at least 2:1 by 10 min after tracer administration (130 min after occlusion). This ratio had increased to 8:1 by 240 min after tracer administration (360 min after occlusion).

The current study also aimed to study the relationship between infarct size determined by ^{99m}Tc -glucarate versus that determined by TTC staining. Previous investigators have examined ^{99m}Tc -glucarate uptake in experimental myocardial infarction in small animal models using rabbits both with and without reperfusion (1). Infarct size on ex vivo images was correlated with infarct size by ^{111}In -antimyosin. The correlation coefficient was 0.76 for the reperfused rabbits and 0.60 for the nonreperfused rabbits. This same laboratory reported a large animal model of 4 dogs undergoing coronary occlusion and reperfusion and then administration of ^{99m}Tc -glucarate and ^{111}In -antimyosin (3). Infarct size was not calculated from images. However, well-counted ^{99m}Tc -glucarate and ^{111}In -antimyosin activities were well correlated. The correlation coefficient was $r = 0.99$. In the clinical study mentioned above, the investigators correlated echocardiogram wall motion abnormalities with ^{99m}Tc -glucarate image abnormalities in patients with acute myocardial infarction (7). They reported that the echocardiogram wall motion abnormality was larger than the ^{99m}Tc -glucarate image abnormality. This difference could be explained by additional stunned myocardium picked up by the echocardiogram technique. However, there was only a weak correlation between the CK levels and the ^{99m}Tc -glucarate abnormality size ($r = 0.53$). Furthermore, there was no correlation between CK levels and intensity of tracer uptake. The current study demonstrated an excellent correlation between infarct size by ^{99m}Tc -glucarate and TTC staining ($r = 0.96$). It should be noted that compared with the Khaw study, our study was based on planimetered infarct size rather than well counts. The current study also demonstrated a linear regression slope near unity.

Our study had the following limitation: It used a canine model of coronary occlusion followed by reperfusion. We selected this model for this initial study since reperfusion therapy is so commonly used clinically in the setting of an acute myocardial infarction. However, a significant number of patients may have contraindications for thrombolytic therapy or may incompletely reperfuse with thrombolytic therapy. Thus, future studies should consider models of persistent coronary occlusion or only partial reperfusion.

The current study has the following clinical implications. Our study, using a large animal model of coronary occlusion and reperfusion, indicates that clinical ^{99m}Tc -glucarate images may be positive as early as 130 min after coronary occlusion when analyzed qualitatively. The study demonstrates that images may be clinically interpretable qualitatively within 30 min and interpretable quantitatively within 10 min after intravenous tracer administration. Image qual-

ity may remain excellent for at least 240 min after tracer administration. Furthermore, this study illustrates that ^{99m}Tc -glucarate imaging may be able to predict relative infarct size.

CONCLUSION

In a large animal model of coronary occlusion and reperfusion, blood ^{99m}Tc -glucarate clearance is triexponential and rapid. There is enhanced tracer uptake and retention in necrotic myocardium as early as 130 min after coronary occlusion. γ -Camera image quality is qualitatively excellent for infarct within 30 min of intravenous tracer administration and remains so for at least 240 min. Images are quantitatively abnormal within minutes of intravenous tracer administration, with hot spot-to-normal zone counts ratios reaching 8:1 at 240 min. Significant differences in myocardial retention are detectable within 10 min of tracer administration. The linear regression relationship between infarct size by ^{99m}Tc -glucarate versus TTC staining is excellent, with $r = 0.96$ and the slope = 0.87.

ACKNOWLEDGMENTS

This study was supported in part by grants from the American Heart Association, the William K. Warren Medical Research Institute, and the Anne and Henry Zarrow Foundation. The authors acknowledge Dr. Koon-Yan Pak from Molecular Targeting Technologies, Inc. (Malvern, PA) for his assistance in providing glucarate kits for the completion of this study. The authors also thank Madelyn Andrews for her expert secretarial assistance. This study is dedicated to the Anne and Henry Zarrow family for their support of medical research, without which these experiments would not have been possible. Ban-An Khaw is a shareholder in Molecular Targeting Technologies, Inc.

REFERENCES

1. Narula J, Petrov A, Pak KY, Lister BC, Khaw BA. Very early noninvasive detection of acute experimental nonreperfused myocardial infarction with ^{99m}Tc -labeled glucarate. *Circulation*. 1997;95:1577-1584.
2. Khaw BA, DaSilva J, Petrov A, Hartner W. In-111 antimyosin and Tc-99m glucaric acid for noninvasive identification of oncotic and apoptotic myocardial necrosis. *J Nucl Cardiol*. 2002;9:471-481.
3. Khaw BA, Atsuko N, O'Donnell SM, Pak KY, Narula J. Avidity of technetium ^{99m}Tc glucarate for the necrotic myocardium: in vivo and in vitro assessment. *J Nucl Cardiol*. 1997;4:283-290.
4. Yaoita H, Fischman AJ, Wilkinson R, Khaw BA, Juweid M, Strauss HW. Distribution of deoxyglucose and technetium- ^{99m}Tc -glucarate in the acutely ischemic myocardium. *J Nucl Med*. 1993;34:1303-1308.
5. Ohtani H, Callahan RJ, Khaw BA, Fishman AJ, Wilkinson RA, Strauss HW. Comparison of technetium- ^{99m}Tc -glucarate and thallium-201 for the identification of acute myocardial infarction in rats. *J Nucl Med*. 1992;33:1988-1993.
6. Beanlands RSB, Ruddy TD, Bielawski L, Johansen H. Differentiation of myocardial ischemia and necrosis by technetium- ^{99m}Tc -glucaric acid kinetics. *J Nucl Cardiol*. 1997;4:274-282.
7. Mariani G, Villa G, Rossettin PF, et al. Detection of acute myocardial infarction by ^{99m}Tc -labeled D-glucaric acid imaging in patients with acute chest pain. *J Nucl Med*. 1999;40:1832-1839.
8. Orlandi C, Crane PD, Edwards DS, et al. Early scintigraphic detection of experimental myocardial infarction in dogs with technetium- ^{99m}Tc -glucaric acid. *J Nucl Med*. 1991;32:263-268.

9. Johnson G, Nguyen KN, Liu Z, Gao P, Pasqualini R, Okada RD. Planar imaging of ^{99m}Tc-labeled (bis(N-ethoxy, N-ethyl dithiocarbamate) nitrido technetium (V)) can detect resting ischemia. *J Nucl Cardiol.* 1997;4:217–225.
10. ten Kate CI, Fischman AJ, Wilkinson RA, et al. Tc-99m-glucaric acid: a glucose analogue [abstract]. *Eur J Nucl Med.* 1990;17:451.
11. Vural I, Narula J, Petrov A, Pak CKY, Khaw BA. Can Tc-99m-glucarate also recognize diffuse myocardial necrosis [abstract]? *J Nucl Med.* 1995;36(suppl):47P.
12. Khaw BA, Rammohan R. Tc-99m glucaric acid targets the nucleoproteins of acutely necrotic myocardium but cannot target myocardial cell death due to apoptosis [abstract]. *Circulation.* 1999;100:I-310.
13. Khaw BA, DaSilva JS, Vora J, Boroujerdi M. Identification of adriamycin cardiotoxicity by two infarct avid agents: In-111 antimyosin and Tc-99m glucaric acid [abstract]. *Circulation.* 1998;98:I-130
14. Khaw BA, Petrov A, Vora JK, Boroujerdi M, Pak KY, Narula J. Tc-99m glucarate is a marker of necrosis: it does not localize in adriamycin induced apoptotic myocardial injury [abstract]. *J Nucl Med.* 1998;29(suppl):159P.
15. Johnson LL, Schofield L, Mastronfrancesco P, Donahay T, Farb A, Khaw BA. Technetium-99m glucarate uptake in a swine model of limited flow plus increased demand. *J Nucl Cardiol.* 2000;7:590–598.
16. Khaw BA, Hartner W, Dasilva J, Pak CKY. 99m-Tc glucarate in imaging acute myocardial infarction: how quickly can infarcts be visualized in vivo [abstract]? *J Nucl Med.* 2001;42(suppl):163P.





The Journal of
NUCLEAR MEDICINE

Early Detection of Infarct in Reperfused Canine Myocardium Using ^{99m}Tc -Glucarate

David R. Okada, Gerald Johnson, Zhonglin Liu, Sonia D. Hocherman, Ban-An Khaw and Robert D. Okada

J Nucl Med. 2004;45:655-664.

This article and updated information are available at:
<http://jnm.snmjournals.org/content/45/4/655>

Information about reproducing figures, tables, or other portions of this article can be found online at:
<http://jnm.snmjournals.org/site/misc/permission.xhtml>

Information about subscriptions to JNM can be found at:
<http://jnm.snmjournals.org/site/subscriptions/online.xhtml>

The Journal of Nuclear Medicine is published monthly.
SNMMI | Society of Nuclear Medicine and Molecular Imaging
1850 Samuel Morse Drive, Reston, VA 20190.
(Print ISSN: 0161-5505, Online ISSN: 2159-662X)

© Copyright 2004 SNMMI; all rights reserved.

 SOCIETY OF
NUCLEAR MEDICINE
AND MOLECULAR IMAGING

The logo for the Society of Nuclear Medicine and Molecular Imaging (SNMMI) features the letters 'S', 'N', 'M', and 'I' in a white, sans-serif font, each contained within a red square. The squares are arranged in a 2x2 grid, with the 'S' and 'N' in the top row and the 'M' and 'I' in the bottom row.